PRAMANA
— journal of
physics

Vol. 42, No. 2,
February 1994
pp. 123–133

Mass asymmetry dependence of fusion time-scales in $^{11}B + ^{237}Np$ and ^{12}C, ^{16}O, $^{19}F + ^{232}Th$ reactions in a dynamical trajectory model

KIRAN KUMAR, R K CHOUDHURY and A SAXENA
Nuclear Physics Division, Bhabha Atomic Research Centre, Bombay 400085, India

MS received 14 June 1993; revised 2 November 1993

Abstract. Dynamical trajectory calculations were carried out for the reactions of $^{11}B + ^{237}Np$ and ^{12}C, ^{16}O and $^{19}F + ^{232}Th$, having mass asymmetries on either side of the Businaro–Gallone critical mass asymmetry α_{BG}, in order to examine the mass asymmetry dependence of fusion reactions in these systems. The compound nucleus formation times were calculated as a function of the partial wave of the reaction for all the systems. This study brings out that for systems with $\alpha < \alpha_{BG}$, the formation times are significantly larger than for $\alpha > \alpha_{BG}$, which is caused by the dynamical effects involved in the large scale shape changes taking place in the fusion process as well as due to the interplay between the thermal and the collective motion during the collision process. The calculated time scales are comparable to the experimental values derived from the pre-fission neutron multiplicity measurements.

Keywords. Heavy ion fusion reactions; time scales; dynamical trajectory model; dependence on mass asymmetry.

PACS No. 25·70

1. Introduction

There have been a number of experimental and theoretical investigations in the past [1–9] to determine the role of the entrance channel mass asymmetry in the fusion dynamics of heavy ion induced reactions. Recently, in the work of Ramamurthy *et al* [4] on the fission fragment angular distributions, it was pointed out that the value of α relative to the liquid drop Businaro-Gallone critical mass asymmetry [10] (α_{BG}) may be important in deciding the fusion path in heavy ion reactions. There have been also some experimental studies to determine the fusion-fission time delay from the studies of pre-scission neutron multiplicities in heavy ion induced reactions which seem to suggest the above behaviour. In the work of Saxena *et al* [6], the fusion-fission time scales were determined for $^{11}B + ^{237}Np$ and ^{11}B, ^{12}C, $^{16}O + ^{232}Th$ systems by measuring the pre-scission neutron multiplicities and it was found that for $^{16}O + ^{232}Th$ system ($\alpha < \alpha_{BG}$) the fusion-fission time is larger than that for $^{11}B + ^{237}Np$, $^{11}B + ^{232}Th$ and $^{12}C + ^{232}Th$ systems ($\alpha > \alpha_{BG}$).

The dynamical threshold for the onset of fusion depends critically on the total charge, orbital angular momentum and mass asymmetry of the system. For mass asymmetric reactions, there are two different saddle points in the potential energy surface [7–9]. The first is the Bohr-Wheeler mass-symmetric saddle point and the second is the conditional saddle point which is obtained with the constraint that mass asymmetry is fixed at the initial value of the reaction. During the fusion reaction,

the target-projectile system is trapped in the valley of the fusion potential, and the dinuclear system drifts along the mass asymmetry co-ordinate by exchange of mass to form a fused nucleus. During this time the inter-nuclear distance R changes because the distance R_P corresponding to the bottom of the pocket in the potential depends on both the mass asymmetry α and angular momentum. The drift along mass asymmetry α will be governed by the potential energy of the quasi-molecular system which has been formed. The total energy calculated with the potential energy $V(R_p)$ taken for several values of initial mass asymmetry α shows that there are two regions of interest: the one corresponds to the system which will drift towards symmetry for $\alpha < \alpha_{BG}$ and the second region corresponds to the system which will drift towards more asymmetric configuration for $\alpha > \alpha_{BG}$. In other words the initial mass asymmetry of the system may have a great influence on the latter development along the mass asymmetry coordinate. There has not been, however, so far detailed dynamical study of the fusion time scales for systems lying on either side of the critical BG point, to bring out clearly the influence of mass asymmetry in such reactions.

The dynamical evolution of the two colliding nuclei can be described by a sequence of shapes which basically consist of two spheres connected by a conical neck. The three macroscopic variables used are: the distance separating the two centres of mass, the neck co-ordinate and the mass asymmetry co-ordinate. The system is then described by the classical equations of motion for obtaining the mean values of the macroscopic variables and their second moments, with the frictional forces taken to be proportional to the velocities in the collective degree of freedom. We have used the formalism of Feldmeier *et al* [11, 12] to study the fusion dynamics of various target projectile systems with mass asymmetries lying on either side of the liquid drop Businaro-Galline critical mass asymmetry. The systems studied are $^{11}B + ^{237}Np$ and ^{12}C, ^{16}O, $^{19}F + ^{232}Th$ reactions for which the fusion-fission time scales have been experimentally deduced from pre-scission neutron multiplicity measurements [6, 13]. It may be noticed that $^{11}B + ^{237}Np$ and $^{16}O + ^{232}Th$ lead to the same compound nucleus, but have mass asymmetries lying on either side of α_{BG}. The calculated values of the fusion time scales are found to compare well with the experimental values. The details of the calculation procedure are given in the section below. Section 3 gives the results and discussion of the calculations and § 4 contains the summary on the present work.

2. Classical dynamical calculations

We use the model of Feldmeier *et al* [11, 12] where the colliding nuclei are treated as two Fermi gases which exchange particles, momentum and entropy through a window in the mean single particle potential. The time development of the collision trajectories are calculated by solving a Langevin equation with a fluctuating dissipative force. The properties of the fluctuating force are determined from a microscopic picture of particle exchange between two nuclei. The macroscopic shapes of the nuclear system are represented by axially symmetric configurations with sharp surfaces. These shapes are uniquely determined by three macroscopic degrees of freedom: the distance between the nuclei s, the neck coordinate σ, and the mass asymmetry Δ defined as:

$$\begin{aligned} s &= \text{distance between two sphere centres} \\ \sigma &= [V_0 - (4\pi/3)R_1^3 - (4\pi/3)R_2^3]/V_0 \\ \Delta &= [R_1 - R_2]/[R_1 + R_2] \end{aligned} \tag{1}$$

where V_0 is the total volume of the system and is independent of $\{s, \sigma, \Delta\}$, R_1 and R_2 are the radii of the two interacting nuclei. If the symmetry axis is taken along z-direction, the shapes of the nuclei can be specified by the profile function $P(s, \sigma, \Delta; z)$ which is defined as [14]

$$P^2(s,\sigma,\Delta;z) = \begin{cases} R_1^2 - z^2 & \text{for} \quad -R_1 \leqslant z \leqslant z_1 \\ a_1 + bz + cz^2 & \text{for} \quad z_1 \leqslant z \leqslant z_2 \\ a_2 + bz + cz^2 & \text{for} \quad z_3 \leqslant z \leqslant z_4 \\ R_2^2 - (z-s)^2 & \text{for} \quad z_4 \leqslant z \leqslant s + R_2 . \end{cases} \tag{2}$$

This representation includes single shapes as well as shapes consisting of two fragments. All the parameters $R_1, R_2, a_1, a_2, b, c, z_1, z_2, z_3, z_4$ depend on the three degrees of freedom defined in (1). In addition there are three rotational degrees of the intrinsic and relative rotation of the di-nuclear complex. Denoting the six macroscopic co-ordinates and their momenta by $(q(t), p(t))$, the Langevin equation can be written as:

$$\begin{aligned} \mathrm{d}\mathbf{p}/\mathrm{d}t &= -\mathrm{d}T/\mathrm{d}\mathbf{q} - \mathrm{d}V/\mathrm{d}\mathbf{q} + \mathbf{X}(t) \\ \mathrm{d}\mathbf{q}/\mathrm{d}t &= M^{-1}\mathbf{p} \end{aligned} \tag{3}$$

where $T = 1/2(\mathbf{p}M^{-1}\mathbf{p})$ denotes the collective kinetic energy and M denotes the mass tensor, while V stands for the conservative potential, and $X(t)$ is the fluctuating force caused by the coupling of the collective degrees of freedom to the intrinsic degrees of freedom. The mass tensor is calculated from the profile function by assuming incompressible and irrotational flow of mass during the shape evolution in the collision. The expression relating the mass parameters to the profile function (eq. (2)) are given in [11]. The potential energy V is calculated by associating with each shape the nuclear and Coulomb energies as follows. The nuclear potential, V_n can be written as a double volume integral of a Yukawa plus exponential folding function [15]:

$$V_n = \frac{-C_s}{8\pi^2 r_0^2 a^3} \int_{\text{shape}} \mathrm{d}^3\mathbf{r}\,\mathrm{d}^3\mathbf{r}' \left(\frac{1}{a} - \frac{2}{|\mathbf{r}-\mathbf{r}'|}\right) \exp\left(-\frac{|\mathbf{r}-\mathbf{r}'|}{a}\right) \tag{4}$$

where

$$c_s = a_s[1 - k_s((N-Z)/A)^2]; \quad a_s = 21{\cdot}7\ \text{MeV}; \quad K_s = 3$$

$$r_0 = 1{\cdot}18\ \text{fm}, \quad a = 0{\cdot}65\ \text{fm}.$$

The Coulomb potential is calculated assuming a uniform charge distribution ρ_c with a sharp surface:

$$V_c = \frac{1}{2}\rho_c^2 \int_{\text{shape}} \mathrm{d}^3\mathbf{r}\,\mathrm{d}^3\mathbf{r}' \frac{1}{|\mathbf{r}-\mathbf{r}'|} \tag{5}$$

The double folding integrals in (4) and (5) are calculated numerically, where the six-fold integral is transformed to a three-fold integral by using a two-fold application of the Gauss divergence theorem for axially symmetric shapes [15]. The energies depend on the three shape degrees of freedom (s, σ, Δ) via the dependence of the profile function $P(q, z)$.

In the above equations, the motion of the system is governed by a strong dissipative force $X(t)$, which is related to the friction and diffusion terms obtained from particle exchange model. One-body dissipation is assumed to be predominant as they have been found to be more relevant for these types of reactions [16].

One-body dissipation: This picture makes use of long mean free path of a nucleon in a nucleus at an excitation energy which is not too high and the mean field of the nucleus acts as a confining vessel. Wall dissipation occurs when particles which are about to hit the wall possess a mean field velocity different from the wall velocity. So after scattering from the wall, their velocity distribution shows a mismatch with the rest of the fluid. The randomisation hypothesis assumes that the bounced particles obtain the velocity distribution of the bulk before they hit the wall again. Window friction occurs for two gases with different velocities in contact at a window. Again particles crossing the window show a mismatch in their velocity distribution with respect to the gas volume in which they are entering. The randomisation assumption implies that the particles have forgotten their original velocity distribution before they return to the window. The fluctuating force $X(t)$ is thus, given by:

$$X(t) = \Sigma R_{ij}(M^{-1}p)_j \tag{6}$$

where R_{ij} is the friction tensor [11]. The energy dissipation rate is given by:

$$\begin{aligned} Q^{\text{wall}} &= \Sigma R_{ij}^{\text{wall}} \dot{q}_i \dot{q}_j \\ Q^{\text{window}} &= \Sigma R_{ik}^{\text{window}} \dot{q}_i \dot{q}_k \\ Q^{\text{w+w}} &= Q^{\text{wall}} + Q^{\text{window}} \end{aligned} \tag{7}$$

As noted earlier, the friction tensor is governed by exchange of nucleons between the interacting nuclei, which results in a fluctuating force (eqn (6)).

To allow a smooth transition between mono and the dinuclear regimes, a form factor f_r is introduced which allows for a smooth transition between the two dissipation mechanisms:

$$Q = (1 - f_r)Q^{\text{w+w}} + f_r Q_{\text{mono}}^{\text{wall}} \tag{8}$$

where the form factor f_r is defined as:

$$f_r(x) = \begin{cases} 0 & 0{\cdot}0 \leqslant x \leqslant 0{\cdot}8 \\ \sin^2\left(\dfrac{x - 0{\cdot}8}{0{\cdot}2}\dfrac{\pi}{2}\right) & 0{\cdot}8 < x < 1{\cdot}0 \\ 1 & x > 1{\cdot}0 \end{cases} \tag{9}$$

where

$$x = \begin{cases} 0 & ; \text{ for separated shapes} \\ R_{\text{neck}}^2/[\min\{R_1^2, R_2^2\}]; & \text{for shapes with neck} \end{cases} \tag{10}$$

The quantity x is a measure of the ratio between the window area and the wall area surrounding a particle in the smaller part of the shape. We have solved the above equations of motion to study the collision trajectories for various values of the partial waves of the reaction. The results of the calculations are presented in the next section.

3. Results and discussion

We have carried out the calculations for the systems of $^{11}B + ^{237}Np$ and ^{12}C, ^{16}O, $^{19}F + ^{232}Th$ at 77, 86, 104 and 114 MeV bombarding energies respectively, corresponding to nearly same compound nuclear excitation energies for all the systems. The equations of motion (eq. (2)) are solved for a given angular momentum 1 to determine the time development of the various macroscopic variables defined in eq. (1). The angular momentum l_{crit}, below which the system fuses, is used to calculate the fusion cross-section. For the above systems, the calculated fusion cross sections agree with the experimental systematics [4] within 10%.

Figures 1(a, b, c) show the dependence of s, σ and Δ as a function of time for the four systems for the angular momentum $1 = 38\,\hbar$, which is close to the fusion critical

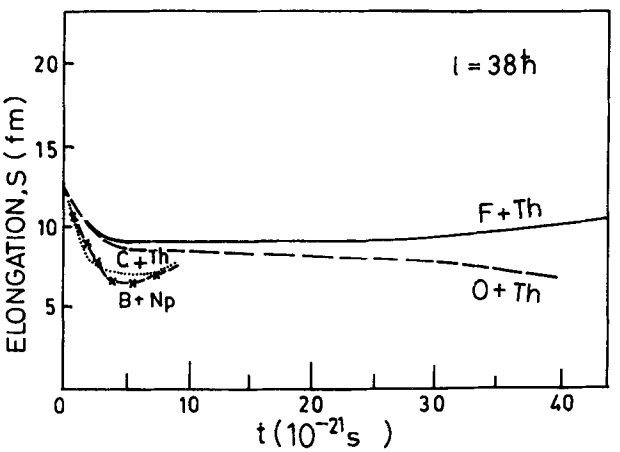

Figure 1a. Time dependence of elongation s for the systems B + Np, C + Th, O + Th and F + Th.

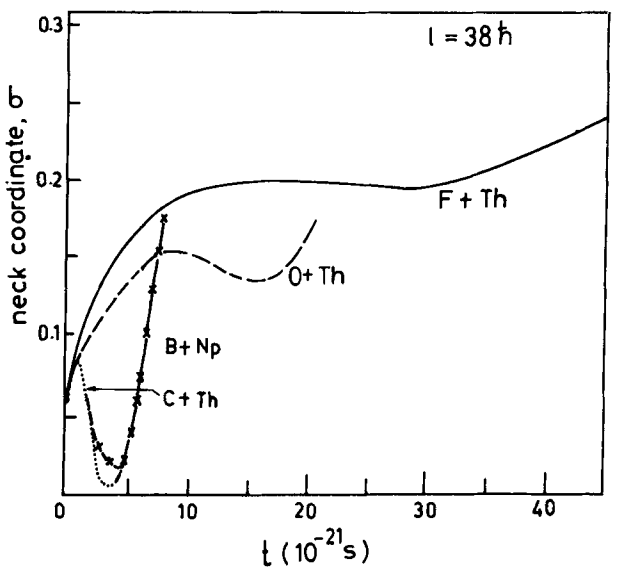

Figure 1b. Same as 1a for neck co-ordinate σ.

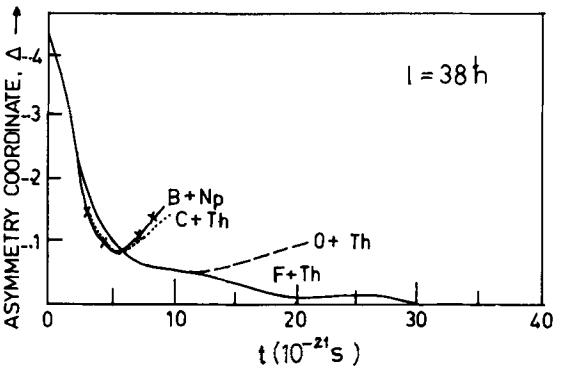

Figure 1c. Same as 1a for asymmetry co-ordinate Δ.

angular momentum l_{crit} for all these target-projectile systems. It is found from figures 1a and 1b that the time development of the elongation and neck coordinates shows quite similar behaviour for the $^{11}B + ^{237}Np$ and $^{12}C + ^{232}Th$ reactions, while for $^{16}O + ^{232}Th$ and $^{19}F + ^{232}Th$ reactions the behaviour is quite different. For the latter cases, there is a significant streching and neck development as the two nuclei fuse, while for $^{11}B + ^{237}Np$ and $^{12}C + ^{232}Th$ reactions, the systems go towards more compact and mononuclear shapes in a shorter time scale. Similarly, as seen from figure 1c, the asymmetry variable Δ decreases sharply with time for $^{16}O + ^{232}Th$ and $^{19}F + ^{232}Th$ systems indicating formation of symmetric shapes while for $^{11}B + ^{237}Np$ and $^{12}C + ^{232}Th$ system Δ shows a minimum value of $-0{\cdot}08$ units at around 5×10^{-21} s and then increases to $-0{\cdot}15$ units before fusion takes place.

Figure 2 shows schematically the time-evolution of the shapes for $l = 38\hbar$ as the two nuclei undergo fusion. This figure brings out clearly differences in the shape evolution as a function of time for the four systems. The fusion time t_{form} (t_{form} is time taken from the beginning of the interaction to compound nucleus formation) for $l = 38\hbar$ is found to be about 8×10^{-21} s for $^{11}B + ^{237}Np$ and $^{12}C + ^{232}Th$ systems, while for the case of $^{16}O + ^{232}Th$ and $^{19}F + ^{232}Th$ systems, it is $\approx 20 \times 10^{-21}$ s and $49{\cdot}3 \times 10^{-21}$ s respectively. As mentioned above, the excitation energies of these systems are roughly same i.e. 59·9, 58·8, 60·8 and 64·0 MeV respectively and one can distinctly visualise the differences in the formation time to be related to the change in the entrance channel mass asymmetry around the B–G mass asymmetry α_{BG}.

Figures 3(a, b, c) shows the typical trajectories in the (s, σ) plane for various l-values for $^{11}B + ^{237}Np$ and ^{16}O, $^{19}F + ^{232}Th$ systems. The numbers indicated are the time taken by the system to reach the end-points in the trajectories. It is seen that for the case of $^{11}B + ^{237}Np$ reaction (figure 3(a)), the mono-nuclear shapes are reached for $l = 38\ \hbar$ and lower l-values, while the system reseparates for $l = 40\hbar$, characterised by deep inelastic behaviour with a very fast transition time of about $0{\cdot}6 \times 10^{-21}$ s. For $^{16}O + ^{232}Th$ and $^{19}F + ^{232}Th$ systems (figures 3b and 3c), the transition between fusion and deep inelastic reactions is not sharply divided in the l-domain. For these systems there is a range of l-values above fusion l-crit for which the composite system goes through substantial amount of stretching and neck formation (being still in the di-nuclear regime) and there is large amount of mass exchange and energy relaxation before the system reseparates into symmetric fragments. For example, as seen from figure 3b, for $^{16}O + ^{232}Th$ system, at $l = 42\hbar$ the neck co-ordinate grows to 0·28 at an elongation of $s = 13$ fm corresponding to the touching distance of the target and

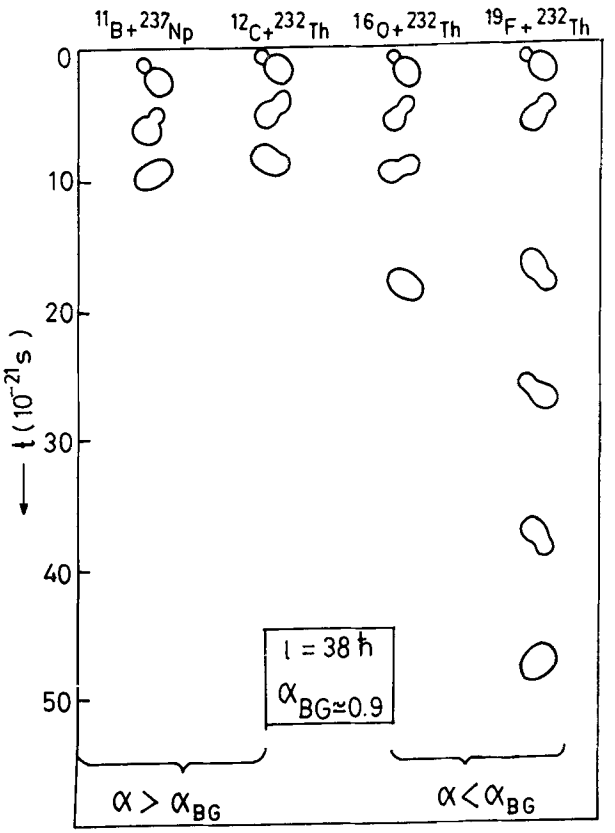

Figure 2. Schematic diagram of the evolution of the nuclear shapes as a function of time.

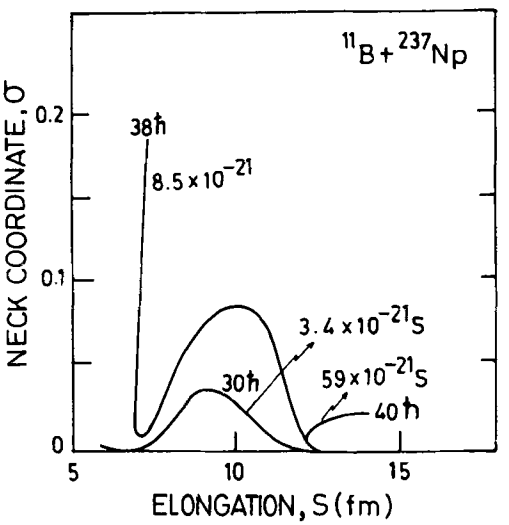

Figure 3a. Typical trajectories in (s, σ) plane for the reaction of B + Np for $l = 30\hbar$, $38\hbar$ and $40\hbar$.

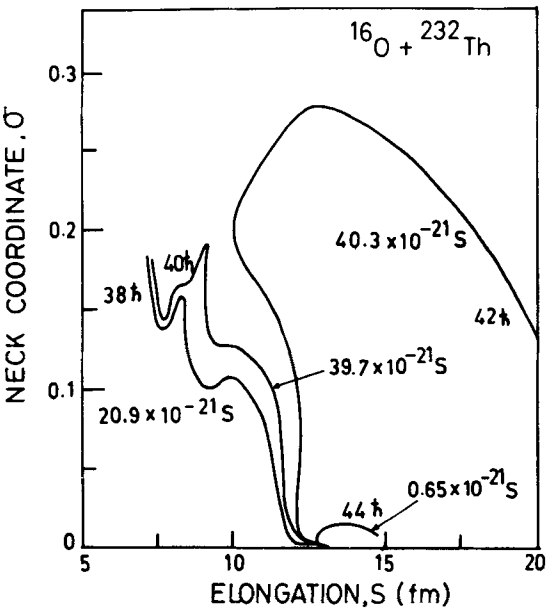

Figure 3b. Same as 3a for O + Th.

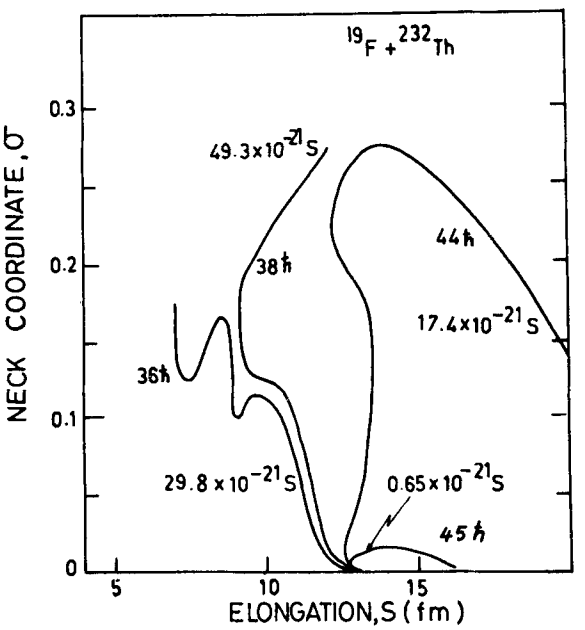

Figure 3c. Same as 3a for F + Th.

projectile, after which the system stretches a lot ($s \approx 20$ fm), and the neck co-ordinate decreases to 0·13 before it fragments into two symmetric pieces. At $l = 44\hbar$, however, the system reseparates very quickly as expected for peripheral deep inelastic type of events. Similar behaviour is also observed for $^{19}F + ^{232}Th$ system for trajectories corresponding to l-values between 40 and $44\hbar$, where a large amount of mass exchange as well as stretching of the di-nuclear system takes place before reseparation

into symmetric fragments. The transition time for $l = 44\hbar$ in $^{19}F + ^{232}Th$ reaction is $17{\cdot}4 \times 10^{-21}$ s indicating that the system undergoes several revolutions, before splitting into two fragments. At $l = 45\hbar$, the system reseparates quickly as a deep inelastic event.

The dependence of t_{form} as a function of the angular momentum of the compound nucleus is shown for all the four systems in figure 4. It is observed that for all l-values, the compound nucleus formation time, t_{form} is higher for $^{16}O + ^{232}Th$ and $^{19}F + ^{232}Th$ systems as compared to that for the other two systems. The compound nucleus formation time averaged over the spin distribution for the $^{11}B + ^{237}Np$ and $^{16}O + ^{232}Th$ reactions, which lead to the same compound nucleus ^{248}Cf are $2{\cdot}86 \times 10^{-21}$ s and 11×10^{-21} s respectively. From the measurement of the pre-scission neutron multiplicities [6], it was observed that $^{16}O + ^{232}Th$ system shows longer fusion-fission time than $^{11}B + ^{237}Np$ system and the differences in the formation time between the

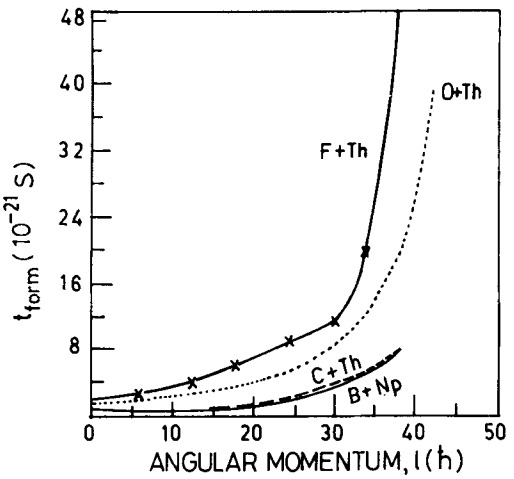

Figure 4. Variation of the compound nucleus formation time with angular momentum for various system.

Table 1. The values of α/α_{BG} are shown in bracket below each system.

	$t_{form}(10^{-21}$ s)			
	B + Np	C + Th	O + Th	F + Th
$1\hbar$	1·02	1·01	0·97	0·94
0	0·56	0·60	1·2	1·73
10	0·72	0·80	2·1	3·13
15	0·90	1·00	2·8	5·21
20	1·20	1·35	4·0	7·52
25	1·80	2·20	5·4	9·32
30	3·40	4·00	8·2	11·02
34	4·80	5·20	12·3	20·19
38	8·00	8·00	20·0	49·30
average t_{form}	$\approx 2{\cdot}86$	3·35	11·00	$17{\cdot}2 \times 10^{-21}$

two systems was found to be $\approx(15 \pm 5) \times 10^{-21}$ s which is in agreement with the present calculation.

Table 1 gives a summary of the results of the calculations for the formation time for all the systems. The values of t_{form} averaged over the l-distribution are also shown in the table. It is clearly seen that for the systems studied, the fusion time scales are larger in case of $\alpha < \alpha_{BG}$ as compared to that with $\alpha > \alpha_{BG}$. It is also observed that the difference in the formation time increases significantly for higher partial waves.

4. Conclusion

The present calculations are based on the particle exchange picture and are found to be very effective in describing the dissipative transport phenomena involved in the heavy ion induced reactions leading to fusion. The applicabibity of this model is, however, confined to beam energies such that the mean field picture is valid for the interaction. Also since the calculation does not incorporate dynamic deforamtion, reactions below the Coulomb barrier cannot be described.

One can apply this model to study the detailed features of the peripheral collisions. The energy loss and mass exchange behaviour in such collisions will, however, be very sensitive to the assumptions of the dissipation mechanism assumed in the model.

The present calculations bring out many new features in the behaviour of the fusion reaction as a function of the initial mass asymmetry of target-projectile system near the liquid drop B–G mass asymmetry (α_{BG}). Firstly, compound nucleus formation time is found to be higher for all the l-values for ^{16}O, $^{19}F + ^{232}Th$ ($\alpha < \alpha_{BG}$) system compared to $^{11}B + ^{237}Np$ and $^{12}C + ^{232}Th$ systems ($\alpha > \alpha_{BG}$). The average compound nucleus formation time (summed over all l-values) is larger by $10–15 \times 10^{-21}$ s for systems having $\alpha < \alpha_{BG}$ as compared to systems with $\alpha > \alpha_{BG}$. Secondly, in the case of ^{16}O, $^{19}F + ^{232}Th$ reactions, there is a range of l-values beyond fusion l_{crit} for which the di-nuclear system undergoes several rotations and large stretching and neck formation before it reseparates into two symmetric fragments. These new class of events can be verified experimentally by carrying out selective measurements of fragment mass and angular distribution as a function of initial angular momentum of the reaction.

In summary, the calculations carried out in the present work show that the liquid-drop Businaro-Gallone mass asymmetry plays an important role in deciding the reaction dynamics and fusion time-scales in the heavy-ion reactions. The partial wave of the reaction has a strong effect on the reaction times in all the systems.

References

[1] B Haas, D Duchene, F A Beck, T Byrski, C Gehringer, J C Merdinger, A Nourredine, V Rauch, J P Vivien, J Barrette, S Tobbeche, E Bozek, J Styczen, J Keinonen, J Dudek and W Nazarewicz, *Phys. Rev. Lett.* **54**, 398 (1985)

[2] A Ruckelshausen, R D Fischer, W Kuhn, V Metag, R Muhlhans, R Novotny, T L Khoo, R V F Janssens, H Groger, D Habs, H W Heyng, R Repnow, D Schwalm, G Duchene, R M Freeman, B Haas, F Haas, S Hlavac, R S Simon, *Phys. Rev. Lett.* **56**, 2356 (1986)

[3] W P Zank, D Hilscher, G Ingold, U Jahnke, M Lehmann and H Rossner, *Phys. Rev.* **C33**, 519 (1986)

[4] V S Ramamurthy, S S Kapoor, R K Choudhury, A Saxena, D M Nadkarni, A K Mohanty, B K Nayak, S V S Sastry, S Kailas, A Chatterjee, P Singh and A Navin, *Phys. Rev. Lett.* **65**, 25(1990)

[5] G Smith, B Hass, A Alderson, I Ali, C W Beausang, M A Bentley, P Dagnall, P Fallon, G de France, P D Forsyth, U Huttmeier, P Romain, D Santos, P J Twin and J P Vivien, *Phys. Rev. Lett.* **68**, 158 (1992)
[6] A Saxena, A Chatterjee, R K Choudhury, S S Kapoor and D M Nadkarni, 1993 *Phys. Rev.* C (in press)
[7] C Gregoire, R Lucas, C Ngo and B Schurmann, *Nucl. Phys.* **A361**, 443 (1981)
[8] K T R Davies and A J Sierk, *Phys. Rev.* **C31**, 915 (1985)
[9] C Gregoire, C Ngoand and E Tomasi, *Nucl. Phys.* **A387**, 37 (1982)
[10] U L Businaro and S Gallone. *Nuovo Cimento* **5**, 315 (1957)
[11] H Feldmeier, *Rep. Prog. Phys.* **50**, 915 (1987)
[12] H Feldmeier and H Spangenberger, *Nucl. Phys.* **A428**, 223c (1984); **A435**, 229 (1985)
[13] J O Newton, D J Hinde, R J Charity, J R Leigh, J J M Bokhorst, A Chatterjee, G S Foote and S Ogaza, *Nucl. Phys.* **A483**, 126 (1988)
[14] J Blocki and W J Swiatecki, Report LBL-12811, (1982)
[15] H J Krappe, J R Nix and A J Sierk, *Phys. Rev.* **C20**, 992 (1979)
[16] J Blocki, R Planeta, J Brzychczyk and K Grotowski, *Z. Phys.* **A341**, 307 (1992)